CHAPTER 44

SEDIMENT THRESHOLD UNDER OSCILLATORY WAVES

Paul D. Komar and Martin C. Miller

School of Oceanography, Oregon State University
Corvallis, Oregon, U.S.A. 97331

ABSTRACT

As the velocity of the water motion near the bottom under oscillatory waves is increased, there comes a stage when the water exerts a stress on the particles sufficient to cause them to move. This study reviews data on threshold of sediment motion under wave action and compares the results with the established curves for threshold under a unidirectional current.

For grain diameters less than about 0.05 cm (medium sands and finer) the threshold is best related by the equation

$$\frac{\rho\, u_m^2}{(\rho_s - \rho)\, g\, D} = 0.21\, (d_o / D)^{1/2}$$

where u_m and d_o are the near-bottom velocity and orbital diameter of the wave motion, ρ is the density of water, and ρ_s and D are respectively the density and diameter of the sediment grains. For grain diameters greater than 0.05 cm (coarse sands and coarser) the equation

$$\frac{\rho\, u_m^2}{(\rho_s - \rho)\, g\, D} = 0.46\pi\, (d_o / D)^{1/4}$$

gives the best prediction of threshold.

Evaluating the drag coefficient with the graph of Jonsson for wave motions, the data on threshold under waves is found to show good agreement with the curves of Shields and Bagnold for the threshold under a unidirectional current.

INTRODUCTION

As the velocity of a fluid flow over a bed of sediments is increased, there comes a stage when the fluid exerts a stress on the particles sufficient to cause them to move from the bed into the flow and be transported. This stage is generally known as the threshold of sediment movement, or as the critical stage for erosion or entrainment. The purpose of this paper is to examine the threshold of sediment motion under oscillatory water-wave motion. This report is an extension of a previous paper [Komar and Miller (1973)], our intent being to first review the findings of that paper and then to compare the results on the threshold under waves with the curves that have been proposed for the threshold under unidirectional currents [Shields (1936); Bagnold (1963)].

Five sets of previously published data will be utilized in the analysis of the threshold. Bagnold (1946) and Manohar (1955) oscillated a bed of sediment through still water within a tank. Besides investigating the threshold, both studies generated ripple marks and vortex water motions which agree with comparable wave channel and prototype observations, indicating the reliability of observations obtained in this manner. Rance and Warren (1969) conducted threshold studies in an oscillating flow water tunnel using material as coarse as 4.8 cm diameter. The advantage of oscillating the bed as in the studies of Bagnold and Manohar, or utilizing the water tunnel as by Rance and Warren is that prototype periods, orbital diameters, and velocities can be obtained. In ordinary wave tanks the periods are generally limited to less than 2 to 3 seconds. However, the threshold data of two such studies is included in this review; Horikawa and Watanabe (1967) and Eagleson, Dean and Peralta (1958). Horikawa and Watanabe utilized a 25 meter long wave tank with wave heights ranging up to 7 cm and periods up to 2.19 sec [maximum bottom orbital velocities up to 8.5 cm/sec]. The Eagleson, Dean and Peralta data is of interest because it consists of the threshold of single isolated grains resting on an otherwise fixed granular bed. Due to page limitations their data will not be presented in the paper; it was found that it did agree with the other sets of

TABLE 1. - Granular Materials Used in Studies of Threshold of Motion

A. Bagnold (1946)

Symbol	material	density, (gm/cm^3)	diameter, D (cm)
+	steel grains	7.90	0.060
●	quartz sand	2.65	0.330
○	quartz sand	2.65	0.080
⊗	quartz sand	2.65	0.036
⌀	quartz sand	2.65	0.016
⊙	quartz sand	2.65	0.009
■	coal	1.30	0.800
◪	coal	1.30	0.250
□	coal	1.30	0.036

B. Manohar (1955)

symbol	material	density, (gm/cm^3)	diameter, D (cm)
ɸ	Del Monte sand No. 2	2.65	0.0280
◒	B.E.B. sand No. 1	2.63	0.0786
⊗	coarse sand No. 1	2.60	0.1006
⊖	coarse sand No. 2	2.60	0.1829
⌀	B.E.B. sand No. 2	2.63	0.1981
▽	glass beads No. 1	2.49	0.0235
▼	glass beads No. 2	2.54	0.0610
△	polyvinyl chloride pellets	1.28	0.317
▲	polystyrene pellets	1.052	0.317

data and supported the conclusions arrived at within this paper.

The available data represents a wide spectrum of sediment types: grain diameters range from 0.009 to 4.8 cm, and densities from 1.052 gm/cm^3 (polystyrene plastic) to 7.90 gm/cm^3 (steel grains). This is summarized in Tables 1 and 2 along with the graphic symbols utilized throughout the paper. A scheme of symbols has been employed to clarify the comparisons; all the varieties of circles signify grains composed of ordinary quartz, the plus symbol (+) is that for steel grains (density greater than quartz), while the triangles, squares, and other miscellaneous shapes represent grains of density lower than quartz (limestones, coal, glass beads, and plastics).

Many equations have been proposed for the threshold of sediment motion under waves; Silvester and Mogridge (1971) present thirteen different equations gathered from the literature. This review will center on the equation presented by Bagnold (1946) and the empirical graph of Rance and Warren (1969), these giving the best results.

TABLE 2. — Granular Materials Used in Study of Threshold by Rance and Warren (1969)

symbol	material	density (gm/cm^3)	diameter, D (cm)
◬	limestone chips	2.72 - 2.55	0.409, 0.777, 1.072, 1.321, 1.387, 1.742, 2.042, 2.515
◇	glass spheres	2.54 - 2.44	0.592, 0.884, 1.186
⬘	concrete cubes	2.39	4.775
◩	coal	1.37 - 1.29	0.706, 1.372, 2.042, 3.251, 4.521
⬙	perspex cubes	1.19	3.200

ANALYSIS

Utilizing the data collected in his experiments, Bagnold (1946) deduced an empirical relationship for the threshold which may be written as

$$\frac{2\pi}{T} = a \left[\frac{\rho_s - \rho}{\rho} g \right]^{1/2} \frac{D^{0.325}}{d_o^{0.75}} \tag{1}$$

where T and d_o are the wave period and near-bottom orbital diameter, D and ρ_s are the grain diameter and density, and g is the acceleration of gravity. This empirical relationship is not dimensionally correct so that the coefficient a is not dimensionless. Utilizing

$$u_m = \frac{\pi d_o}{T} \tag{2}$$

for the maximum horizontal velocity u_m associated with the orbital bottom motion, equation (1) can be algebraically manipulated to

$$\frac{\rho u_m^2}{(\rho_s - \rho) g D} = a' (d_o / D)^{1/2} D^{0.15} \tag{3}$$

which is dimensionless except for the residual $D^{0.15}$ factor. Dropping this factor leaves the dimensionally correct relationship

$$\theta_t' = \frac{\rho u_m^2}{(\rho_s - \rho) g D} = a'' (d_o / D)^{1/2} \tag{4}$$

which is shown in Figure 1 along with the data of Bagnold (1946). The straight-line fit yields $a'' = 0.21$ in equation (4). Inclusion of the $D^{0.15}$ factor decreases the data scatter but the straight-line fit does not quite pass through the origin.

Figure 2 utilizes the data obtained by Manohar (1955) to test the relationship of equation (4). Manohar collected data for both laminar and turbulent boundary layers whereas Bagnold indicated that his boundary

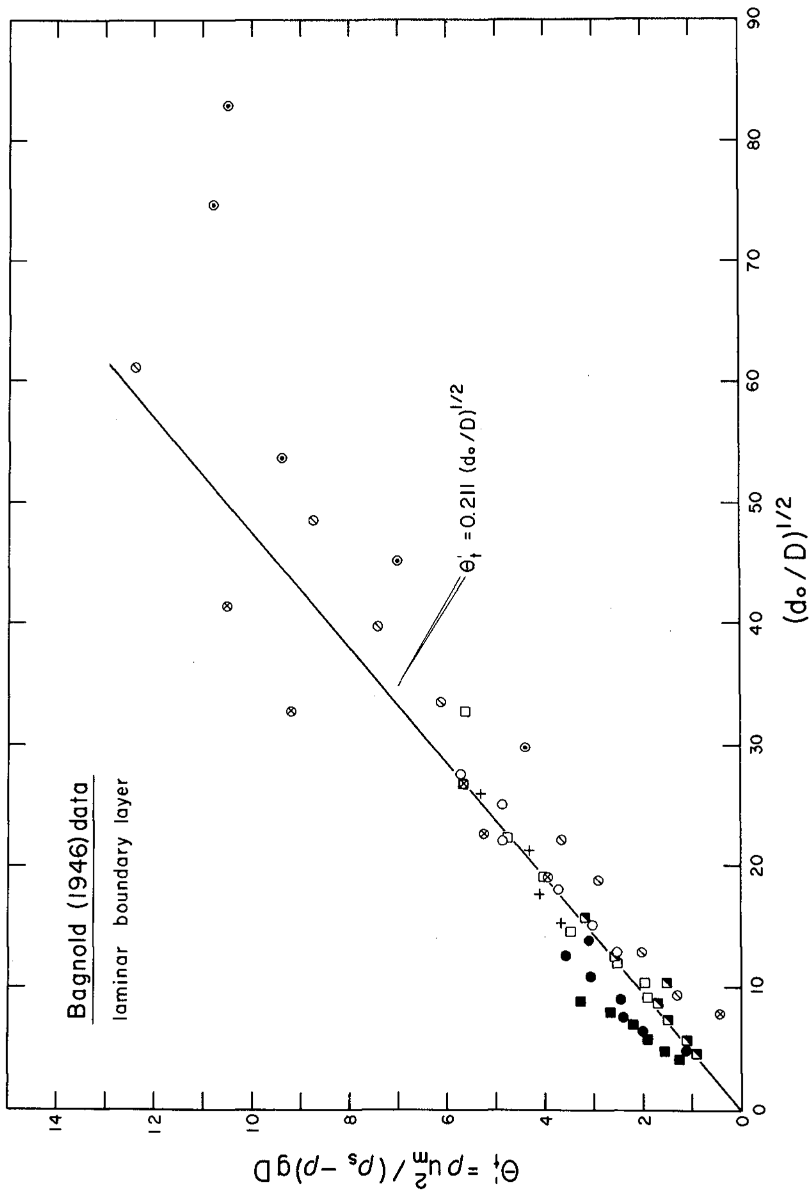

Figure 1: An examination of equation (4) using the data of Bagnold (1946). Symbols are defined in Table 1.

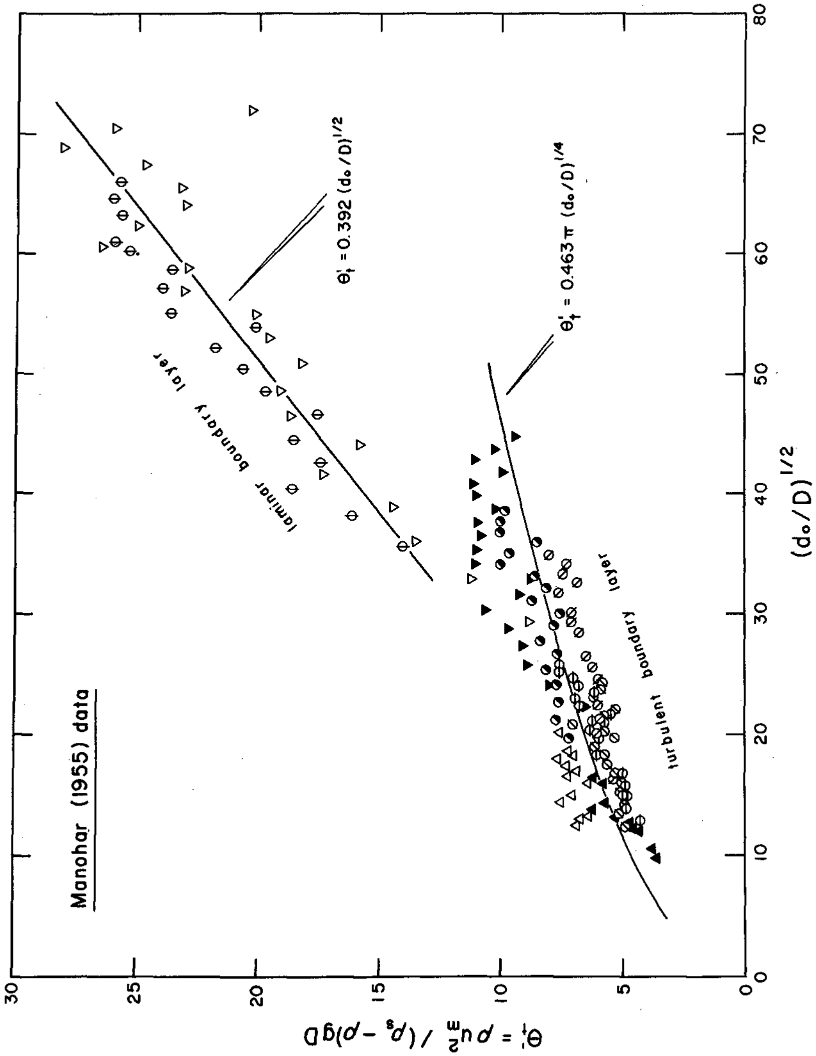

Figure 2: An examination of equation (4) using the data of Manohar (1955). Symbols are defined in Table 1.

layer was laminar in all cases. It is seen in Figure 2 that Manohar's data with a laminar boundary layer yields a good straight-line relationship which gives $a'' = 0.39$ in equation (4). This value for a'' is higher than the value obtained with the data of Bagnold (1946). Determining when the threshold of sediment movement has been achieved and sufficient grain movement occurs is rather subjective and in all probability this difference in a'' values between the two sets of data results from this personal difference between the observers' judgements.

The wave tank data of Horikawa and Watanabe (1967) yields $a'' = 0.3$ in equation (4), just about the average of the values from the Bagnold and Manohar data. However, the Horikawa and Watanabe data shows a better trend if d_0/D is to the 1st power in equation (4) rather than to the 1/2 power. The choice for the value of a'' in equation (4) will be discussed again later in this paper.

Also apparent in Figure 2 is that when the boundary layer is turbulent the data follows no systematic trend according to equation (4). Another relationship for the threshold under a turbulent boundary layer is required. Rance and Warren (1969) found good empirical trends between the ratio d_0/D and the dimensionless number $\rho u_m/(\rho_s - \rho)gT$ which represents the ratio of the acceleration forces to the effective gravity force acting on a grain. Their experiments were for coarse grains in which the boundary layer would be turbulent. Figure 3 plots the data of Manohar (1955) obtained in a turbulent boundary layer against these dimensionless ratios. It is seen that there is a very smooth trend, grains of widely differing diameters and densities agreeing. Also shown is a curve which is based on the data trends as given in Rance and Warren (1969, Fig. 1); it is clear that there is a remarkable agreement between the data of Manohar and that of Rance and Warren. The data of Eagleson, Dean and Peralta (1958) is also in agreement. The graph of Figure 3 can therefore be used to evaluate the threshold conditions of sediment movement when the boundary layer is turbulent.

The essentially straight line of Figure 3 yields the equation

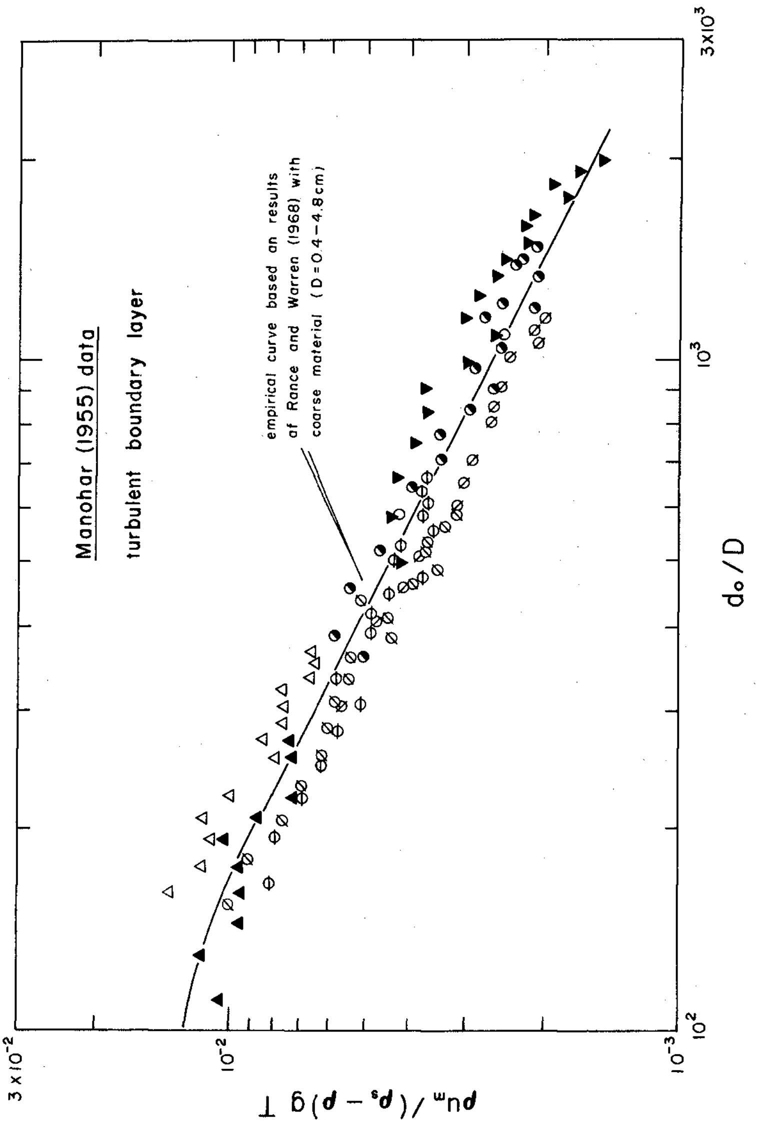

Figure 3: A comparison of the threshold data of Manohar (1955) for a turbulent boundary layer with the empirical curve of Rance and Warren (1969). Symbols defined in Table 1.

$$\frac{\rho\, u_m}{(\rho_s - \rho)\, g\, T} = 0.463 \Big/ (d_o/D)^{0.75} \tag{5}$$

Again utilizing equation (2), equation (5) becomes

$$\frac{\rho\, u_m^2}{(\rho_s - \rho)\, g\, D} = 0.463\pi\, (d_o/D)^{1/4} \tag{6}$$

which is very similar to equation (4) except that d_o/D is to the 1/4 power. This equation is shown in Figure 2 compared to the coarse grain data of Manohar, plotting as a parabola.

In summary, we found that when the grain size is small and the boundary layer is apparently laminar equation (4) can be used to evaluate the threshold condition under waves, and when the grain size is coarse and the boundary layer turbulent the empirical curve of Figure 3 or equations (5) or (6) can be used. In our preceeding paper [Komar and Miller (1973)] we further analyzed the data with respect to the nature of the boundary layer. We concluded that for grain diameters less than about 0.05 cm (medium sands and finer) the sediment threshold is reached before individual grains shed eddies and therefore the boundary layer is laminar. Under these conditions equation (4) applies. For grain diameters greater than 0.05 cm (coarse sands and coarser) the individual exposed grains shed eddies prior to reaching threshold so that the boundary layer is essentially turbulent when the threshold is finally achieved. This would agree with the observations of Bagnold and Manohar on the nature of their boundary layers. However, comparisons with the Reynolds numbers and so on that have been proposed for determining the conditions of the boundary layer were inconclusive. The value of δ/D where δ is the thickness of the boundary layer, is uncertain due to the uncertainty in the evaluation of δ. The transition appears to occur at approximately $\delta/D = 0.1$ to 0.3, depending on whose equation for δ you use. The critical grain size of 0.05 cm is the same as that found in the threshold of sediment motion under unidirectional steady currents; it is the position of the minimum in the threshold curve such as that presented by Bagnold (1963) [see Figure 5 of this paper]. The causes for the division at this critical 0.05 cm diameter are therefore probably the same. When graphed in the proper format, equations (4) and (6) give a similar appearance to curves derived theoretically by Carstens, et. al (1969) although the magnitudes of the values differ. This is taken to indicate basic agreement with their theoretical developments on the threshold under waves.

COMPARISONS WITH UNIDIRECTIONAL FLOW THRESHOLD

In this section we shall compare the results for the threshold under oscillatory motions with the established curves for threshold under a unidirectional steady current. The left sides of equations (3), (4) and (6), denoted by θ_t', are seen to be very similar to the relative stress

$$\theta = \frac{\tau}{(\rho_s - \rho)\, g\, D} = \frac{0.5\, f\, \rho\, u_m^2}{(\rho_s - \rho)\, g\, D} \tag{7}$$

employed by Shields (1936), Bagnold (1963), and others in the unidirectional threshold. All that is required is that θ_t' or ρu_m^2 be multiplied by $0.5f$, where f is a drag coefficient such that we obtain the stress $\tau = 0.5\, f\, \rho\, u_m^2$. Jonsson (1967, Figure 6) provides the necessary graph for the evaluation of the friction factor f for wave motions. He demonstrates that f is a function of the Reynolds number $u_m(0.5d_o)/\nu$, ν being the viscosity, and the parameter $(0.5d_o)/D$. For each of the many data sets we have evaluated these parameters, utilizing the graph of Jonsson to obtain f, finally giving the θ_t value of equation (7). This then can be compared to the results for unidirectional flow.

Shields (1936) related θ_t to $u_* D/\nu$, where $u_* = \sqrt{\tau/\rho}$, for the unidirectional flow data. Figure 4 presents just such a graph with the Shields curve and the data on oscillatory flow threshold.

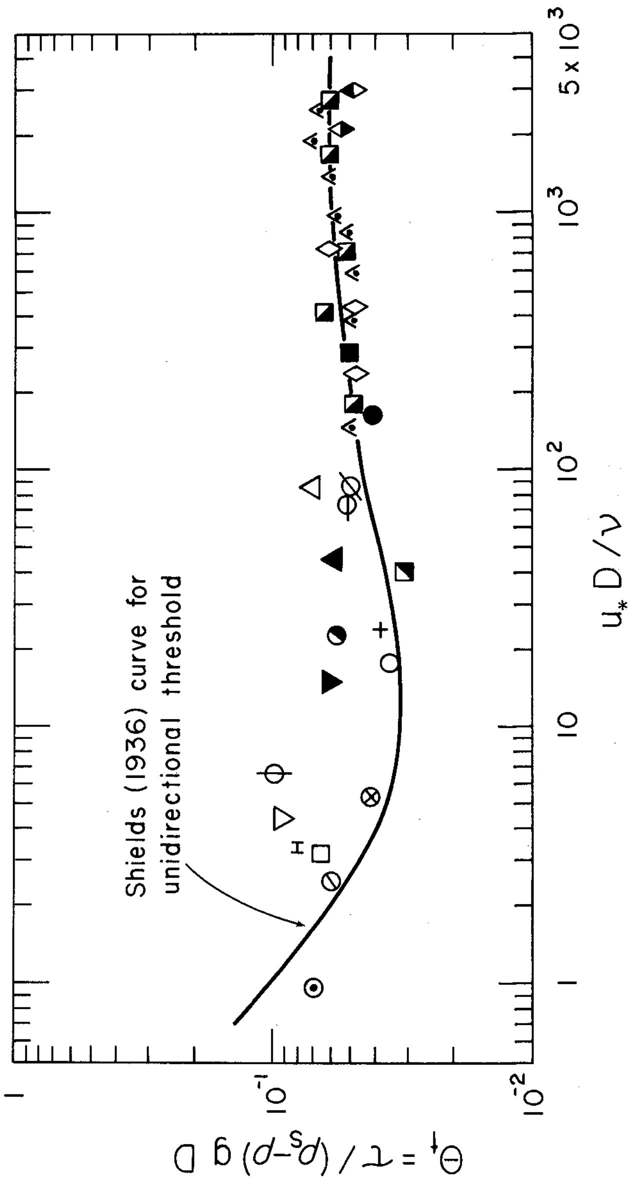

Figure 4: Comparison between the Shields curve for threshold under unidirectional currents and the threshold data for oscillatory wave motions. Symbols are defined in Tables 1 and 2. The H symbol is for the data of Horikawa and Watanabe (1967).

The first fact of interest is that individual sets of data for a given grain size and density plot as essentially a single point. Figures 1, 2 and 3 spread the data out according to wave period and orbital diameter (or velocity), whereas in Figure 4 the data for a given grain D and ρ_s plots in a single position. This indicates that the drag coefficient f adequately accounts for the effects of the wave periodicity on the drag stress. The agreement between the data and the right limb of the curve is particularly good. The data is mainly that of Rance and Warren (1969). The data on the left half of the graph is more scattered but this is due principally to the systematic differences between the results of Bagnold (1946) and Manohar (1955). The Bagnold data is seen to agree better with the Shields unidirectional curve while the Manohar data is displaced above the curve. It should be pointed out that the degree of scatter is comparable to the scatter in the original data from unidirectional flow upon which the curve was originally based. Utilizing the Bagnold data alone, Madsen and Grant (in press) have similarly demonstrated agreement with the Shields curve.

From a practical standpoint, the Shields graph is particularly difficult to employ since it relates the threshold to $u_* D/\nu$. For this reason, Bagnold (1963) represented it as θ_t versus the grain diameter D directly. Such a graph is presented in Figure 5 along with the oscillatory flow threshold data. Again there is good agreement on the right limb of the curve and more scatter on the left, the Bagnold data showing best agreement on the left. Strictly speaking, only the quartz data should have been plotted in the graph. In order to go from the Shields curve of Figure 4 to the curve of Figure 5, Bagnold (1963) had to assume the grains had the density of quartz. In spite of this it is seen that the other density grains show fair agreement with the curve.

For the laminar boundary layer Jonsson (1967, p. 134) gives

$$f = 2\left[\frac{u_m\,(0.5\,d_o)}{\nu}\right]^{-1/2} \qquad (8)$$

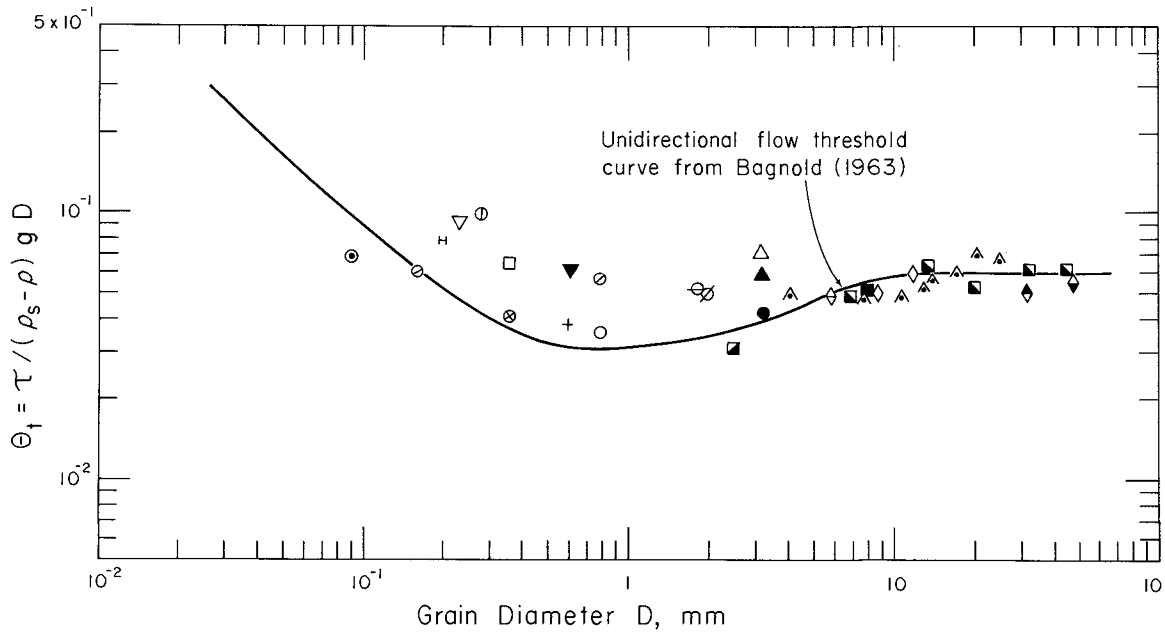

Figure 5: Comparison between the Bagnold (1963) curve for threshold under unidirectional flow and the threshold data for oscillatory wave motions. Symbols defined in Tables 1 and 2 except for H which signifies data of Horikawa and Watanabe (1967).

for the drag coefficient. Multiplying equation (4) by this gives

$$\theta_t = \frac{\tau_t}{(\rho_s - \rho)\, g\, D} = \frac{a''\sqrt{2}}{\left(\dfrac{u_m D}{\nu}\right)^{1/2}} \tag{9}$$

suggesting that a plot of θ_t versus the Reynolds number $u_m D/\nu$ might be most logical for the case of the oscillatory threshold. Such a plot is shown in Figure 6. The heavy curve shown is our own interpretation as to the best fit to the data as such a graph has not been previously presented. Also shown are the straight lines according to equation (9) with $a'' = 0.21$ (from the Bagnold data alone), and with $a'' = 0.30$ (the average of the Bagnold and Manohar results). The heavy curve is made to approach the straight line where $a'' = 0.21$ since the Bagnold data gave the best comparisons to the Shields and Bagnold (1963) curves for unidirectional threshold.

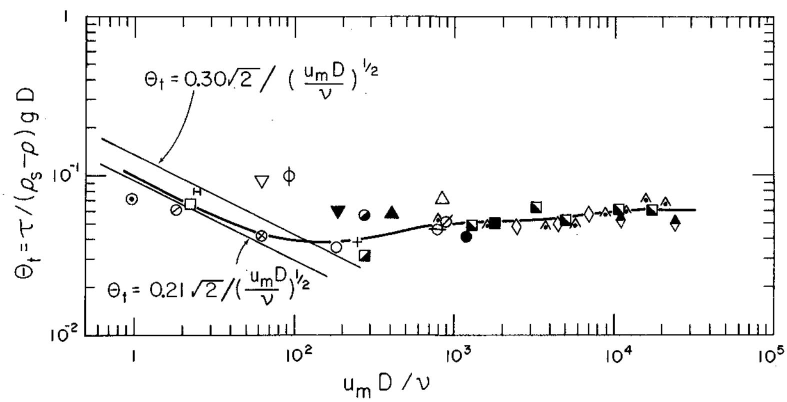

Figure 6: Threshold θ_t versus the Reynolds number $u_m D/\nu$. Symbols defined in Tables 1 and 2.

PRACTICAL EVALUATION OF THRESHOLD UNDER WAVES

Given a grain diameter D and density ρ_s, it is difficult to employ Figures 4 and 6 to estimate the threshold under waves. This is because $u_* D/\nu$ and $u_m D/\nu$ contain the fluid flow characteristics as well as the sediment diameter. Figure 5 is somewhat better in that the threshold is related directly to D alone. Application of this figure yields the stress τ_t for threshold which can in turn give the bottom orbital velocity u_m for sediment movement. This requires evaluation of the drag coefficient f from the graph of Jonsson (1967) which is also not a straight-forward procedure. It is apparent that a simpler approach would be to go directly to equations (4) and (6), the equation depending on whether the grain size is larger or smaller than 0.05 cm. Doing this avoids any evaluation of the drag coefficient. The approach can be simplified even further when it is recognized that for oscillatory wave motions the threshold for a given grain D and ρ_s can be specified by a wave period T and orbital velocity at the bottom u_m. This is shown graphically in Figure 7, based on the two equations. The graph does assume $\rho_s = 2.65$ gm/cm^3 and so applies only to normal quartz sands. For $D > 0.05$ cm, equation (6) is employed and it is seen that there is a set of curves, one for each wave period. The higher the period the greater the orbital velocity u_m required for threshold. For $D < 0.05$ cm, equation (4) is utilized with $a'' = 0.21$, obtained from the Bagnold data alone. More study is required on the best value for this a'' coefficient; this value was selected in part on the basis of the agreement between the Bagnold data and the curves of Shields (1936) and Bagnold (1963) shown above. It is seen in Figure 7 that there is some difficulty in joining the curves in the region of $D = 0.05$ cm. At high periods ($T \geqslant 10$ sec) they do join smoothly, but at lower periods they are offset and we have had to join them by dashed curves indicating a compromise in the results. For periods $T \leqslant 5$ seconds there will be some uncertainty as to the u_m for the threshold of grain sizes on the order of $D = 0.05$ cm obtained with Figure 7 or the basic equations. Under these circumstances it may be best to utilize Figure 5,

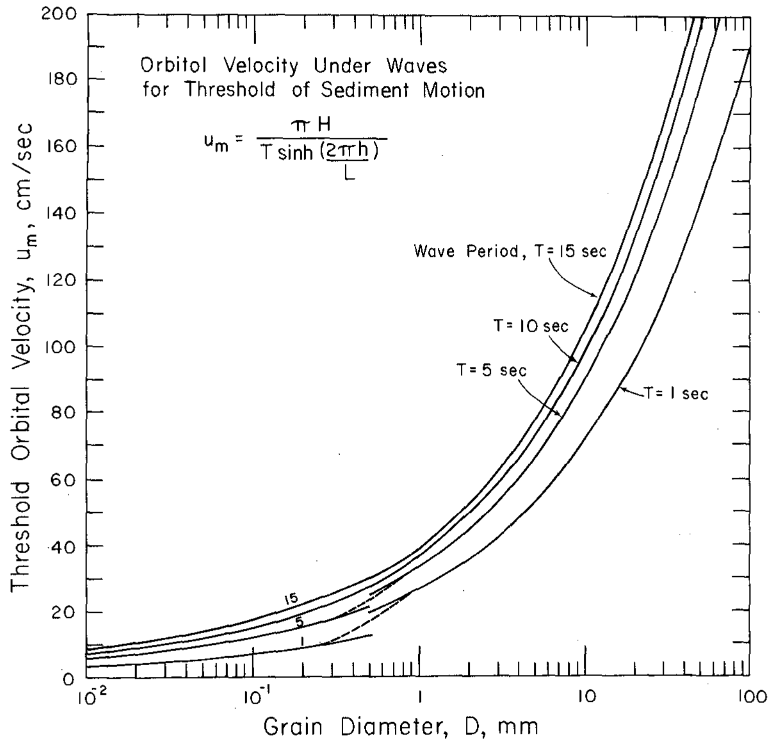

Figure 7: The near-bottom orbital velocity u_m for sediment threshold under waves.

but even there it is apparent that there must be considerable uncertainty as to the exact position of the curve.

The graph of Figure 7 has the obvious advantage that it is very straight-forward to employ, yielding the wave period T and bottom orbital velocity u_m necessary for sediment threshold. There are of course many combinations of water depth h, wave period T, and wave height H, that could yield the required velocity u_m.

Probably the most severe short-coming to the results presented here is the total lack of field data as to the threshold under waves.

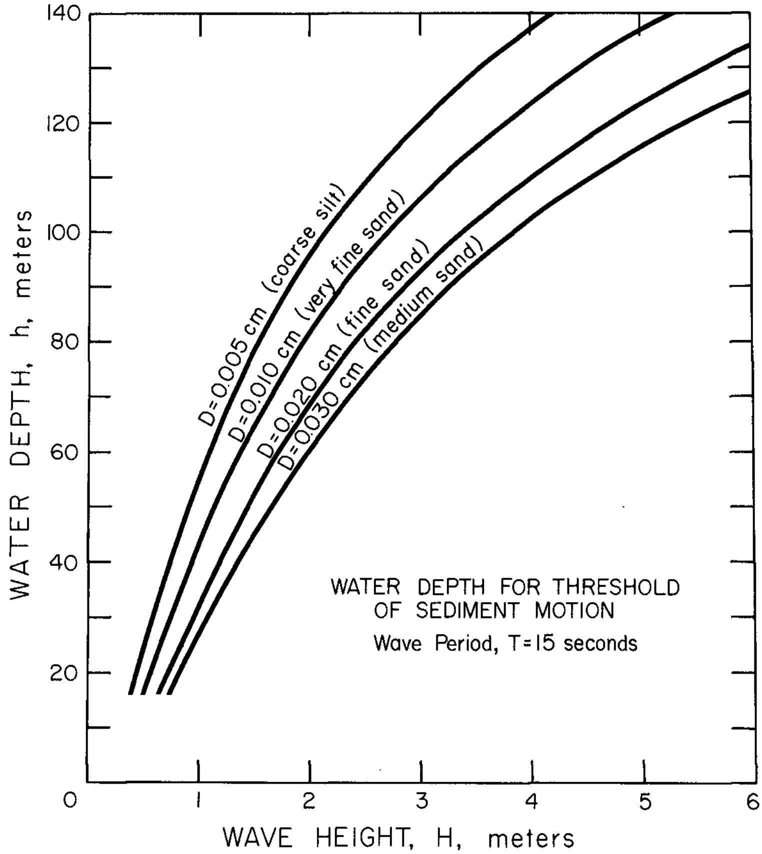

Figure 8: The water depth to which the sediment grain sizes shown can be placed in motion by waves of period 15 seconds.

The difficulties involved in obtaining such observations are apparent. We do have some indications of threshold under waves from the observations of symmetrical oscillatory ripple marks on continental shelves. For example, we (Komar, Neudeck and Kulm, 1972) have found such ripples in bottom photographs on the Oregon continental shelf in water depths as great as 125 meters, sometimes deeper. Figure 8 gives the expected water depth of sediment motion for a wave period $T = 15$ seconds and a range of grain diameters and wave heights. These curves are based on the above threshold equations. It is seen that expected wave heights would be capable of moving the bottom sediments and producing the observed ripple marks at 125 meters water depth on the Oregon shelf. As discussed by Silverster and Mogridge (1971), equations of the sort presented in this paper can be expected to give conservative results as to the depth of sediment motion in the oceans. The most important effects might be that interactions of wave trains of slightly differing period would generate higher instantaneous velocities, and small protruberances on the bed could cause sediment motion at lower velocities than implied by the analysis. The conservative nature of the equations was another reason for our selection of $a'' = 0.21$ in equation (4) rather than 0.30 obtained from an average of all the data. Before we can make proper estimates of the threshold of sediment motion under real ocean wave conditions, some of these effects must be more thoroughly investigated.

ACKNOWLEDGMENTS

This research was supported by the Oceanography Section, National Science Foundation, NSF Grant GA-36817.

REFERENCES

Bagnold, R. A. (1946) Motion of waves in shallow water, Interaction between waves and sand bottom: Proc., Royal Society London, series A, v. 187, p. 1-15.

Bagnold, R. A. (1963) Mechanics of marine sedimentation: in *The Sea*, edited by M. N. Hill, Interscience Publ., p. 507-582.

Carstens, M. R., F. M. Neilson, and H. D. Altinbilek (1969) Bed forms generated in the laboratory under an oscillatory flow: Analytical and experimental study: U.S. Corps of Engineers, Coastal Engineering Research Center, Tech. Memo. No. 28, 39 p.

Eagleson, P. S., R. G. Dean, and L. A. Peralta (1958) The mechanics of the motion of discrete spherical bottom sediment particles due to shoaling waves: U.S. Army Corps of Engineers, Beach Erosion Board, Tech. Memo. No. 104, 55 p.

Horikawa, K., and A. Watanabe (1967) A study of sand movement due to wave action: Coastal Engineering in Japan, v. 10, p. 39-57.

Jonsson, I. G. (1967) Wave boundary layers and friction factors: Proc. 10th Conf. on Coastal Engr., p. 127-148.

Komar, P. D., R. H. Neudeck, and L. D. Kulm (1972) Observations and significance of oscillatory ripple marks on the Oregon continental shelf: in *Shelf Sediment Transport*, edited by Swift, Duane and Pilkey, Dowden, Hutchinson & Ross, Inc., Stroundsburg, Pa., p. 601-619.

Komar, P. D., and M. C. Miller (1973) The threshold of sediment movement under oscillatory water waves: Jour. Sedimentary Petrology, v. 43, p. 1101-1110.

Komar, P. D., and M. C. Miller (in press) On the comparison between the threshold of sediment motion under waves and unidirectional currents with a discussion of the practical evaluation of the threshold: Journal Sedimentary Petrology.

Madsen, O. S., and W. D. Grant (in press) The threshold of sediment movement under oscillatory waves: A discussion: Jour. Sedimentary Petrology.

Manohar, Madhav (1955) Mechanics of bottom sediment movement due to wave action: U.S. Army Corps of Engineers, Beach Erosion Board, Tech. Memo. No. 75, 121 p.

Rance, P. J., and N. F. Warren (1969) The threshold movement of coarse material in oscillatory flow: Proc. 11th Conf. on Coastal Engr., p. 487-491.

Shields, A. (1936) Anwendung der Ahnlichkeits Mechanik und der Turbulenzforschung auf die Geschiebe Bewegung: Preuss. Versuchanstalt fur Wasserbau und Schiffbau, Berlin, 20 p.

Silvester, R., and G. R. Mogridge (1971) Reach of waves to the bed of the continental shelf: Proc. 12th Conf. on Coastal Engr., p. 651-667.